

## Hugoniot Data for Carbon at Megabar Pressures

D. Batani,<sup>1</sup> F. Strati,<sup>1</sup> H. Stabile,<sup>1</sup> M. Tomasini,<sup>1</sup> G. Lucchini,<sup>1</sup> A. Ravasio,<sup>1</sup> M. Koenig,<sup>2</sup> A. Benuzzi-Mounaix,<sup>2</sup> H. Nishimura,<sup>3</sup> Y. Ochi,<sup>3</sup> J. Ullschmied,<sup>4</sup> J. Skala,<sup>4</sup> B. Kralikova,<sup>4</sup> M. Pfeifer,<sup>4</sup> Ch. Kadlec,<sup>4</sup> T. Mocek,<sup>4</sup> A. Präg,<sup>4</sup> T. Hall,<sup>5</sup> P. Milani,<sup>6</sup> E. Barborini,<sup>6</sup> and P. Piseri<sup>6</sup>

<sup>1</sup>*Dipartimento di Fisica "G. Occhialini," Università degli Studi di Milano Bicocca and INFN, Piazza della Scienza 3, 20126 Milano, Italy*

<sup>2</sup>*Laboratoire pour l'Utilisation des Lasers Intenses, UMR 7605 CNRS-CEA-Ecole Polytechnique-Paris VI, Palaiseau, France*

<sup>3</sup>*ILE, Osaka University, 2-6 Yamadaoka, Suita City, Osaka 565-0871, Japan*

<sup>4</sup>*PALS Research Centre, Za Slovankou 3, 18221 Prague 8, Czech Republic*

<sup>5</sup>*University of Essex, Wivenhoe Park, Colchester CO4 3SQ, United Kingdom*

<sup>6</sup>*Dipartimento di Fisica, Università degli Studi di Milano and INFN, Via Celoria 16, 20133 Milano, Italy*

(Received 2 September 2003; published 13 February 2004)

We present an experimental point for the carbon equation of state (EOS) at megabar pressures, obtained by laser-driven shock waves. The rear side emissivity of "two-materials two-steps" targets (Al-C) was recorded with space and time resolution and, by applying the impedance mismatch method, allowed a direct determination of relative EOS points. Experiments were performed at the PALS and LULI laboratories using carbon samples with two different values of initial density, in order to explore a wider region of the phase diagram. Previously unreachable pressures were obtained. The results are compared with previous experiments and with available theoretical models and seem to show a high compressibility of carbon at megabar pressures.

DOI: 10.1103/PhysRevLett.92.065503

PACS numbers: 64.30.+t, 52.38.-r

The equation of state (EOS) of carbon at high pressures (megabar or multimegabar regime) is of interest for several branches of physics.

**Material science:** Carbon is a unique element due to its polymorphism and the complexity and variety of its state phases. The EOS of carbon has been the subject of several recent important experimental and theoretical scientific works [1–15]. The important phenomenon of carbon metallization at high pressure has long been predicted theoretically but until now never experimentally proved. At very high pressures the regime of nonideal strongly correlated and partially degenerate plasmas is approached, which is characterized by an almost complete absence of experimental data [15–18].

**Astrophysics:** The description of high-pressure phases is essential for developing realistic models of planets and stars [19,20]. Carbon is a major constituent (through methane and carbon dioxide) of giant planets such as Uranus and Neptune. High pressures are thought to produce methane pyrolysis with a separation of the carbon phase and the possible formation of a diamond or metallic layer [21–23]. Metallization of the carbon layer in the mantle of these planets (the "ice layers") could give a high electrical conductivity and, by the dynamo effect, be the source of the observed large magnetic fields [24,25].

Concerning carbon metallization, the first theoretical estimates (Van Vechten [1]) set the triple point for the transition among diamond ( $\alpha$ ), liquid metal ( $\beta_l$ ), and solid metal ( $\beta_s$ ) at 1.7 Mbar and 3100 K, a prediction not in agreement with experimental results by Shaner *et al.* [2] and Grover [3]. More recent works set the metallic transition at much larger pressures: Yin and

Cohen [4] predict a transition from diamond to a BC-8 semimetallic phase at  $\approx 11$  Mbar (and a second transition to a SC-4 metallic phase at  $\approx 27$  Mbar), in fair agreement with the calculations by Biswas *et al.* [5], who put the upper limit of diamond stability at  $\approx 12$  Mbar, and with the calculations by Fahy and Louie [6] ( $\approx 11.1$  Mbar). Ruoff and Luo [7], working on experimental data on gap closure by Mao *et al.* [8], put the metallic transition at  $\approx 8.4$  Mbar. Such pressures can easily be generated in the laboratory by using laser-driven shocks.

At higher temperatures, liquid phases are predicted, going from nonmetallic at low pressures to semimetallic and metallic as the pressure is increased. The first experimental evidence of a liquid metallic phase was given by Bundy [9]. Nowadays, the most accepted phase diagram of carbon by Grumbach and Martin [10] sets the structural changes in liquid carbon at pressures of 4 and 10 Mbar. This suggests that laser-driven shocks ( $P = 2\text{--}6$  Mbar,  $T > 20\,000$  K) should reach a liquid metallic phase. In Fig. 1 we report a simplified version of the Grumbach-Martin phase diagram to which we added the Hugoniot curves corresponding to the initial densities  $\rho_0 = 1.6$  and  $1.45$  g/cm<sup>3</sup> (the two values used in our experiment). Again, the liquid metallic phases can easily be reached with laser shocks. These are, indeed, nowadays the only laboratory tool which can achieve pressures of a few tens of megabars [18].

In this Letter, we present the first Hugoniot data for carbon obtained with laser-driven shocks. In recent years, it has been well established that laser shocks are a useful tool for high-pressure physics, to compress materials at megabar pressures and measure their EOS

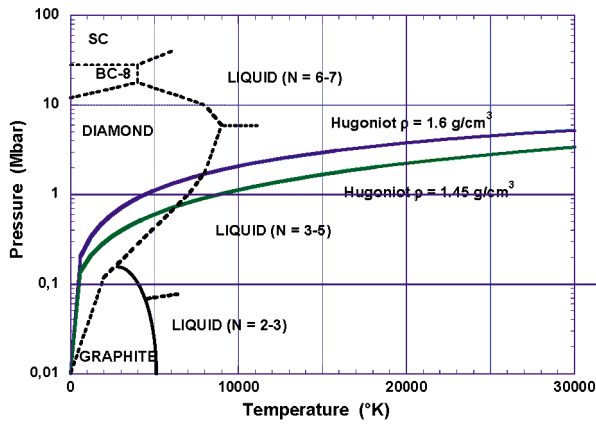


FIG. 1 (color online). Grumbach-Martin phase diagram (after [12]) and the two Hugoniot curves corresponding to the initial densities  $\rho_0 = 1.6$  and  $1.45$  g/cm<sup>3</sup>.

[26,27]. The goal of our experiment was to begin the exploration of carbon EOS in the pressure range 1–15 Mbar. We got the first experimental points at pressures higher than 8 Mbar. Moreover, we substantially increased the number of EOS data for carbon at pressures  $>1$  Mbar (here we present nine new EOS points against a total of about 20 points which, to our knowledge, were available in literature [28–32]).

One general limitation of shock-wave EOS experiments is that only data on the Hugoniot curve of the material are obtained. This is because of the fact that shocks compress and heat the material at the same time, so pressure and temperature are no longer two independent variables. One way to overcome such a limitation is to use a sample with a reduced density  $\rho_0$  (porous or foam target). This changes the initial conditions in the material so that data along *different* Hugoniot curves are obtained. Hence, by changing  $\rho_0$  the whole EOS plane can be explored. In particular, by reducing the initial density  $\rho_0$  of the sample, the same shock pressure  $P$  will correspond to a higher temperature  $T$  (internal energy  $E$ ) and a reduced final density  $\rho$ .

The experiment is based on generating high quality shocks and using “two steps–two materials” targets (Fig. 2). Relative EOS data of “unknown” materials (here C) are obtained by using a “well-known” reference (here Al). Al behavior at high pressure is well known, making it a typical reference material for shock experiments. The method is described in detail in Refs. [27].

Some laser shots were done at LULI where three laser beams at  $\lambda = 0.53$   $\mu\text{m}$  were focused at intensities of  $\approx 5 \times 10^{13}$  W/cm<sup>2</sup>. The pulse was Gaussian in time with a full width at half maximum (FWHM) of 600 ps. In order to increase laser energy (and shock pressure), other shots were done with the PALS iodine laser [33], with typical energy of 250 J per pulse at a wavelength of 0.44  $\mu\text{m}$ , focused up to  $2 \times 10^{14}$  W/cm<sup>2</sup>. The pulse was Gaussian with a FWHM of 450 ps. In both cases, large

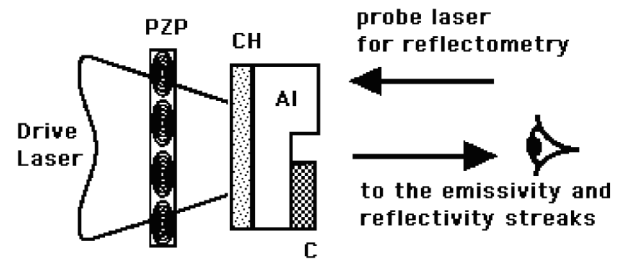


FIG. 2. Scheme of the experimental setup. The CH layer may be (or may not be) present in order to reduce x-ray emission from the laser irradiated side. The probe laser, used at LULI only, was a Nd:YAG converted to  $2\omega$  with pulse duration of 8 ns.

focal spots and phase zone plates [26] were used to get uniform laser illumination and avoid 2D effects in the propagation of the shock.

Two diagnostics systems (Fig. 2), based on streak cameras coupled to photographic objectives and 12 bit charge coupled device cameras, were used: (a) rear side time resolved imaging (to record target self-emissivity), and (b) time resolved visible reflectometry (at LULI only). Both diagnostics allow the measurements of the shock breakout times from the base and steps of the “two steps–two materials” target (see Fig. 2). Hence, we measured the shock velocity in Al and C simultaneously on the same laser shot. Details on the experimental setup are reported in Ref. [34] for PALS, and in [26] for LULI (and for the reflectivity diagnostics in Ref. [35]). Time and spatial resolution of both diagnostics, in both laboratories, were typically of the order of 10 ps and 10  $\mu\text{m}$ .

The reflectivity temporal behavior is important since it can provide evidence of insulator to metal transitions (optical reflectivity is directly related to the density of free charge carriers in the material [35]). However, this requires a different target configuration, and no attempt was made in this direction in this first experiment.

Targets, and, in particular, the carbon layers, are an important part of the experiment. Some carbon depositions were done at the University of Milan using the supersonic cluster beam deposition technique with appropriate masks [36] which allows quite uniform layers and steep steps to be deposited. The particular deposition system allows carbon to stick on Al avoiding the usual delamination problems. More important, it is possible to deposit carbon layers with a density variable between 1 and 2 g/cm<sup>3</sup>. In our experiment, carbon layers with initial density  $\rho_0 = 1.45 \pm 0.10$  g/cm<sup>3</sup> were used. Figure 3 shows a scanning electron microscope (SEM) photo of the carbon steps deposited on a CH/Al substrate, at the University of Milan. The deposition technique allowed the realization of targets with an acceptable surface roughness (less than 0.5  $\mu\text{m}$ , i.e.,  $\approx 3\%$  of step thickness which was of the order of 15  $\mu\text{m}$ ). These give an error comparable to the typical  $\leq 5\%$  due to streak-camera resolution. The Al step thickness was 5  $\mu\text{m}$ .

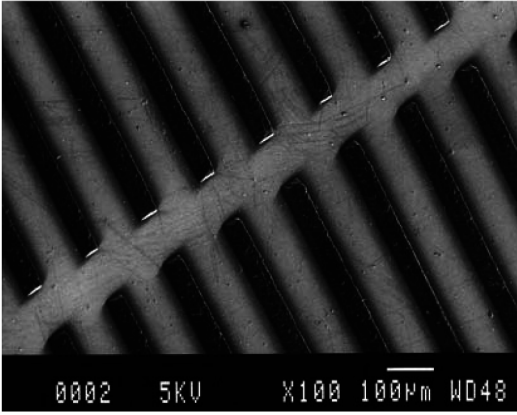


FIG. 3. SEM image of carbon steps with  $\rho_0 = 1.45 \text{ g/cm}^3$  deposited on a CH/Al substrate. Al steps are not present since they were deposited later.

Other carbon targets were fabricated at General Atomics [37] using a completely different technique based on the use of colloidal carbon. In this case, carbon with initial density  $\rho_0 = 1.6 \pm 0.10 \text{ g/cm}^3$  was produced. Stepped targets were made of lathe machining of bulk aluminum. The Al base was  $\approx 8 \mu\text{m}$ , and the step thickness was  $\approx 8.5 \mu\text{m}$ . The carbon layer was then produced and the target was machined again to produce the C step (with thickness  $\approx 10 \mu\text{m}$ ). The use of two different types of targets allows a comparison of measurements and a better confidence in our results.

Figure 4 shows typical results obtained from the emissivity diagnostics. In total we obtained five good experimental points at LULI (two for  $\rho_0 = 1.45 \text{ g/cm}^3$  and three for  $\rho_0 = 1.6 \text{ g/cm}^3$ ) and four good points at PALS (all for  $\rho_0 = 1.6 \text{ g/cm}^3$ ). These are shown in Fig. 5 with all the other experimental results already available in the literature in the pressure range  $P \geq 1.5 \text{ Mbar}$ . Data, grouped according to their initial density  $\rho_0$ , are compared to the shock polar curve derived from the SESAME tables (the model QEOS [38] yields practically identical results for carbon, even if usually it does

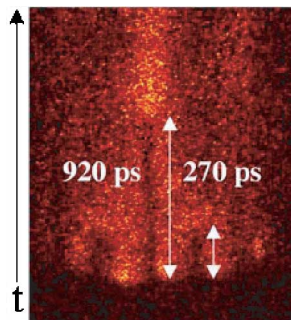


FIG. 4 (color online). Shock breakout streak image of the target rear side in emission. Shot energy was 25.3 J. Arrows indicate the shock breakout from the Al step (right) and from the C step (left). The size of the image is  $600 \mu\text{m} \times 1.7 \text{ ns}$ .

not describe the Hugoniot with the same accuracy as the SESAME EOS does).

The errors on pressure and fluid velocity are  $\approx 20\%$  and  $\approx 15\%$ , respectively; these error bars have been estimated by calculating the propagation of experimental errors on shock velocity (5%) on the quantities determined by the mismatch method. The error on shock velocity is instead determined from the experimentally measured uncertainties on step thickness and by streak-camera temporal resolution.

All our data, for both initial densities, are below the shock polar curve derived from the SESAME tables. Despite our quite large error bars (which make most points compatible with the theoretical curve), such results show a systematic deviation, and indicate a compressibility of carbon, at these pressures, much higher than what is predicted by most models [the density  $\rho$  of the compressed sample is obtained from the Hugoniot Rankine relations for shocks, namely, from  $\rho(D - U) = \rho_0 D$ ]. However, such behavior could also be due to the presence of systematic errors in our experiment. One possible cause often cited for explaining errors in laser-shock EOS experiments is preheating induced by x rays. In our case, preheating was surely small for the points at LULI because of the rather low laser intensity and the presence of a CH layer on the laser irradiated side, which reduces x-ray generation (as shown experimentally in [35]). On the contrary, for the shots at PALS preheating was measured by calibrating the emissivity diagnostics and, for the two shots at higher energy (pressure), it was as high as a couple of eV [34]. Despite this, the LULI points are as far from SESAME as the PALS points. Therefore,

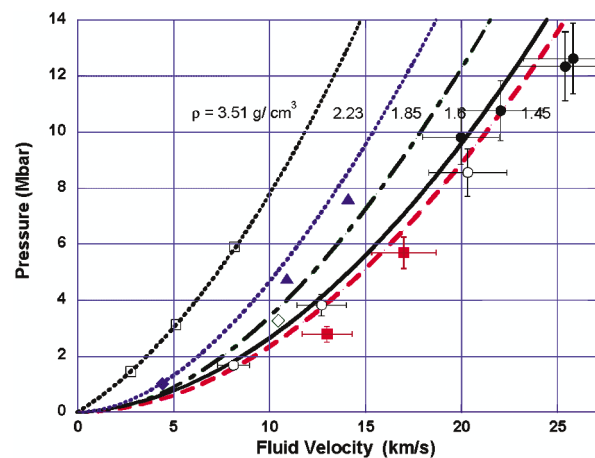


FIG. 5 (color online). Experimental EOS results from shock experiments. Only data with  $P \geq 1.5 \text{ Mbar}$  and corresponding Hugoniot are shown. Our points: full squares,  $1.45 \text{ g/cm}^3$  LULI; empty circles,  $1.6 \text{ g/cm}^3$  LULI; full circles,  $1.6 \text{ g/cm}^3$  PALS. Previous points: empty diamond,  $1.85 \text{ g/cm}^3$ , Pavlovskii *et al.* [28]; triangles,  $2.2 \text{ g/cm}^3$ , Nellis [29]; full diamond,  $2.23 \text{ g/cm}^3$ , Pavlovskii *et al.* [28]; empty squares,  $3.51 \text{ g/cm}^3$  (diamond), Pavlovskii [30].

preheating is probably not the cause of deviation from theoretical curves (or at least not of the whole deviation). Another possible systematic effect could be due to the high porosity of the targets, even if porous and foam targets are routinely used in EOS experiments. Hence, even if this point requires further future work and analysis, for the moment we can conclude that at very high pressures carbon is likely to be more compressible than predicted by SESAME or QEOS. Let us notice that a deviation from SESAME is also observed for other points obtained at high shock pressure (for instance, the point at  $\approx 3$  Mbar for carbon with  $\rho_0 = 1.85$  g/cm<sup>3</sup> reported by Pavlovskii and Drakin [28]). Even more interestingly, the same behavior was observed by Nellis *et al.* [29] who, using underground nuclear explosions as a compression tool, report two EOS points for graphite ( $\rho_0 = 2.2$  g/cm<sup>3</sup>) at 4.76 and 7.61 Mbar.

The relation between shock velocity  $D$  and fluid velocity  $U$  for carbon in the megabar range is linear ( $D = C + SU$ , where  $C$  is the sound velocity in the material in that pressure range). For carbon with  $\rho_0 = 1.6$  g/cm<sup>3</sup>, from SESAME (or QEOS), we get  $C \approx 5$  km/s and  $S \approx 1.27$  [39]. A linear interpolation of our points instead yields  $S \approx 1.08$ – $1.14$  (depending on whether we consider or not the two “preheated” points). From this we get an “experimental” shock polar  $P = \rho_0 DU = r_0 U(C + SU)$  which, of course, nicely interpolates our results in the  $(P, U)$  plane. Such a curve is above the thermodynamic limit  $P = \rho_0 U^2$  corresponding to infinite compressibility (all our experimental points are above such a limit). However, it seems too close to the shock polar for a perfect gas, which again could indicate an influence from systematic effects. For the case  $\rho_0 = 1.45$  g/cm<sup>3</sup> we did not make any attempt to determine  $S$  since we had two points only.

The observed increased compressibility of carbon suggests that at a given pressure along the Hugoniot, the density in the final liquid state (see Fig. 1) is smaller than that for solid. Transitions to less dense phases also enhance thermal contributions, explaining the observed pressure discrepancy. This agrees with the conclusions by Nellis *et al.* [29] and reinforces their observations.

The authors thank the technical staffs of LULI and PALS for help in running the experiments; C. Olivotto, E. Henry, T. Desai, M. Moret (Milano Bicocca), and S. Alba (ST, Agrate Brianza), for the work on target characterization; J. Meyer-ter-Vehn and A. Kemp for the availability of the QEOS code (in the version MPQEOS developed at MPQ). This work was supported by the European Union under the action “Transnational Access to Major Research Infrastructures” of the Improving Human Potential (IHP) program of the 5th FP.

[1] J. A. Van Vechten, Phys. Rev. B **7**, 1479 (1973).

- [2] J.W. Shaner, J.M. Brown, D.A. Swenson, and R.G. McQueen, J. Phys. (Paris), Colloq. **45**, 235 (1984).
- [3] R. Grover, J. Chem. Phys. **71**, 3824 (1979).
- [4] M.T. Yin and M.L. Cohen, Phys. Rev. Lett. **50**, 2006 (1983); M.T. Yin, Phys. Rev. B **30**, 1773 (1984).
- [5] R. Biswas *et al.*, Phys. Rev. B **30**, 3210 (1984).
- [6] S. Fahy and S.G. Louie, Phys. Rev. B **36**, 3373 (1987).
- [7] A.L. Ruoff and H. Luo, J. Appl. Phys. **70**, 2066 (1991).
- [8] H.K. Mao and P.M. Bell, Science **200**, 1145 (1978).
- [9] F.P. Bundy, Physica (Amsterdam) **156A**, 169 (1989); J. Geophys. Res. **85**, 6930 (1980); Nature (London) **241**, 116 (1973).
- [10] M. Grumbach and R. Martin, Phys. Rev. B **54**, 15730 (1996).
- [11] T. Sekine, Appl. Phys. Lett. **74**, 350 (1999).
- [12] L. Benedetti *et al.*, Science **286**, 100 (1999).
- [13] S. Scandolo *et al.*, Phys. Rev. B **53**, 5051 (1996).
- [14] A. Cavalleri *et al.*, Europhys. Lett. **57**, 281 (2002).
- [15] In this regime, the most complete EOS are the SESAME tables developed at the Los Alamos Laboratory (SESAME Report on the Los Alamos Equation-of-State library, Report No. LALP-83-4, T4 Group LANL, Los Alamos, 1983).
- [16] M. Ross, Rep. Prog. Phys. **48**, 1 (1985).
- [17] S. Eliezer, A. Ghatak, and H. Hora, *Equation of State: Theory and Applications* (Cambridge University Press, Cambridge, 1986).
- [18] Y. Gupta and S. Sharma, Science **277**, 909 (1997).
- [19] S. Saumon *et al.*, Astrophys. J. Suppl. Ser. **99**, 713 (1995).
- [20] T. Guillot, Science **286**, 72 (1999).
- [21] M. Ross, Nature (London) **292**, 435 (1981).
- [22] F. Ancillotto *et al.*, Science **275**, 1288 (1997).
- [23] W.J. Nellis *et al.*, J. Chem. Phys. **107**, 9096 (1997); W.J. Nellis *et al.*, Science **240**, 779 (1988).
- [24] N.F. Ness *et al.*, Science **246**, 1473 (1989); N.F. Ness *et al.*, Science **233**, 85 (1986).
- [25] J.E. Connerney *et al.*, J. Geophys. Res. **92**, 15329 (1987).
- [26] M. Koenig *et al.*, Phys. Rev. E **50**, R3314 (1994).
- [27] M. Koenig *et al.*, Phys. Rev. Lett. **74**, 2260 (1995); D. Batani *et al.*, Phys. Rev. B **61**, 9287 (2000); D. Batani *et al.*, Phys. Rev. Lett. **88**, 235502 (2002).
- [28] M.N. Pavlovskii and V.P. Drakin, JETP Lett. **4**, 116 (1966).
- [29] W.J. Nellis *et al.*, J. Appl. Phys. **90**, 696 (2001).
- [30] M.N. Pavlovskii, Fiz. Tverd. Tela (Leningrad) **13**, 893 (1971).
- [31] W.H. Gust, Phys. Rev. B **22**, 4744 (1980).
- [32] *LASL Shock Hugoniot Data*, edited by S.P. Marsch (University of California, Berkeley, 1980), pp. 28–51.
- [33] K. Jungwirth *et al.*, Phys. Plasmas **8**, 2495 (2001).
- [34] D. Batani *et al.*, Phys. Rev. E **68**, 067403 (2003).
- [35] A. Benuzzi *et al.*, Phys. Plasmas **5**, 2410 (1998).
- [36] E. Barborini *et al.*, J. Phys. D **32**, L105 (1999); E. Barborini *et al.*, Appl. Phys. Lett. **77**, 1059 (2000); P. Piseri *et al.*, Rev. Sci. Instrum. **72**, 2261 (2001).
- [37] Special thanks to J. Kaae, General Atomics, San Diego, CA, USA, for target fabrication.
- [38] R.M. More *et al.*, Phys. Fluids **31**, 3059 (1988).
- [39] This is true for QEOS and the SESAME table 7830. Other carbon tables give different, but close, values.